



How Water-Aggregate Interactions Affect Concrete Creep: Multiscale Analysis

Muhammad Irfan-ul-Hassan¹; Markus Königsberger²; Roland Reihnsner³; Christian Hellmich, M.ASCE⁴; and Bernhard Pichler, Aff.M.ASCE⁵

Abstract: Customary micromechanics models for the poroelasticity, creep, and strength of concrete restrict the domain affected by the hydration reaction to the cement paste volume, considering the latter as a thermodynamically closed system with respect to the (chemically inert) aggregate. Accordingly, the famous Powers hydration model appears to be a natural choice for the determination of clinker, cement, water, and aggregate volume fractions entering such micromechanical models. The situation changes once internal curing occurs, i.e., once part of the water present is absorbed initially by the aggregate, and then is sucked back to the cement paste during the hydration reaction. This paper develops an extended hydration model for this case, introducing water uptake capacity of the aggregate and paste void-filling extent as additional quantities. Based on constant values for just these two new quantities, and on previously determined creep properties of cement pastes as functions of an effective water:cement mass ratio (i.e., that associated with the cement paste domain rather than with the entire concrete volume), a series of ultrashort-term creep tests on different mortars and concretes can be very satisfactorily predicted by a standard microviscoelastic mathematical model. This further extends the applicability range of micromechanics modeling in cement and concrete research. DOI: [10.1061/\(ASCE\)NM.2153-5477.0000135](https://doi.org/10.1061/(ASCE)NM.2153-5477.0000135). © 2017 American Society of Civil Engineers.

Author keywords: Creep homogenization; Continuum micromechanics; Correspondence principle; Cement paste; Upscaling; Internal curing.

Introduction

Concrete hydration is generally regarded as a process from which the aggregate, being chemically inert, is fully excluded, and which therefore takes place exclusively in the cement paste, where water reacts with cement grains to form hydrates. Correspondingly, concrete hydration models such as the famous Powers–Acker–Hansen model (Powers and Brownyard 1946; Acker and Ulm 2001; Jensen and Hansen 2001) are typically built on evolving volume fractions of cement clinker, water, and hydrates in the cement paste, and, considering the cement paste compartment as a thermodynamically closed system, all these volume fractions can be traced back to the hydration degree and to the (initial) water:cement mass ratio.

By contrast, the volume fractions of cement paste and aggregate remain constant at the hierarchical level of concrete. In addition to other applications, such hydration models have been a particularly appropriate basis for the development of multiscale mechanics models for concrete, whether related to elasticity (Bernard et al. 2003; Hellmich and Mang 2005; Sanahuja et al. 2007), poroelasticity (Ulm et al. 2004; Ghabezloo 2010), viscoelasticity (Scheiner and Hellmich 2009), or strength (Pichler and Hellmich 2011; Pichler et al. 2013).

All these models have been experimentally validated to different levels of precision, so that on the one hand, multiscale continuum mechanics has become an accepted theoretical tool in cement and concrete research, yet on the other hand, the field is still open for improvements. The latter is true in particular for the very challenging topic of concrete creep, which spans several orders of time magnitude, from the scale of minutes (Vandamme and Ulm 2009; Delsaute et al. 2012; Boulay et al. 2012; Vandamme and Ulm 2013; Zhang et al. 2014; Irfan-ul-Hassan et al. 2016) to that of several days (Bažant et al. 1976; Tamtsia et al. 2004; Rossi et al. 2012), weeks (Tamtsia and Beaudoin 2000; Laplante 2003; Atrushi 2003; Briffaut et al. 2012), months (Rossi et al. 1994; Zhang et al. 2014), or even years (Bažant et al. 2011, 2012; Zhang et al. 2014).

This paper shows that the challenge in the multiscale modeling of concrete creep probably does not lie so much in finding the appropriate micromechanical representation of the material, but rather in the reliable estimation of the evolving volume fractions of the material constituents, used by the corresponding micromechanics models as input. In this context, the authors (1) abandoned the aforementioned assumption of the cement paste being a thermodynamically closed system, and (2) explicitly introduced water migration from the interaggregate space into the aggregate, as well as back-suction of water from the aggregate into the hydrating (and therefore water-consuming) cement paste.

¹Ph.D. Student, Institute for Mechanics of Materials and Structures, TU Wien–Vienna Univ. of Technology, Karlsplatz 13/202, A-1040 Vienna, Austria. ORCID: <https://orcid.org/0000-0002-5970-6927>. E-mail: muhammad.irfan-ul-hassan@tuwien.ac.at

²Ph.D. Student, Institute for Mechanics of Materials and Structures, TU Wien–Vienna Univ. of Technology, Karlsplatz 13/202, A-1040 Vienna, Austria. E-mail: markus.koenigsberger@tuwien.ac.at

³Postdoctoral Researcher, Institute for Mechanics of Materials and Structures, TU Wien–Vienna Univ. of Technology, Karlsplatz 13/202, A-1040 Vienna, Austria. E-mail: roland.reihnsner@tuwien.ac.at

⁴Professor and Chair, Institute for Mechanics of Materials and Structures, TU Wien–Vienna Univ. of Technology, Karlsplatz 13/202, A-1040 Vienna, Austria. E-mail: christian.hellmich@tuwien.ac.at

⁵Associate Professor, Institute for Mechanics of Materials and Structures, TU Wien–Vienna Univ. of Technology, Karlsplatz 13/202, A-1040 Vienna, Austria (corresponding author). E-mail: bernhard.pichler@tuwien.ac.at

Note. This manuscript was submitted on June 29, 2016; approved on June 22, 2017; published online on November 2, 2017. Discussion period open until April 2, 2018; separate discussions must be submitted for individual papers. This paper is part of the *Journal of Nanomechanics and Micromechanics*, © ASCE, ISSN 2153-5434.

The paper is organized as follows. A simple mathematical model for water migration into and from the aggregate was formulated in the section on Modeling Hydration-Dependent Water Migration to and from Aggregate. Based on the initial water:cement mass ratio, the hydration degree, and two newly introduced quantities—the water uptake capacity of the aggregate and the water-filling extent of the cement paste voids—this model provides the volume fractions of water, cement clinker, hydrates, and aggregate within concretes and mortars with water-absorbing aggregate. These volume fractions then were used in a micromechanical model for mortar and concrete creep, upscaling cement paste behavior, as quantified in ultrashort-term tests by Irfan-ul-Hassan et al. (2016), to the mortar and concrete level, as detailed in the section “Creep Homogenization of Mortars and Concretes.” Corresponding micromechanical model predictions were then compared with 32 newly performed ultrashort-term creep tests of two different mortars and two different concretes, which were made from the same cement but differ in water:cement and aggregate:cement mass ratios, in the section “Comparison of Ultrashort Creep Experiments and Corresponding Micromechanics Predictions: Identification of Water Absorption Capacities of Quartz Aggregate and of Paste Void-Filling Extent.” It is checked whether this comparison would allow for identification of one value each for (1) the water uptake capacity of aggregate; and (2) the cement-specific void-filling extent by water sucked out from the aggregate. In addition, air entrapment during mixing of concrete is considered.

Modeling Hydration-Dependent Water Migration to and from Aggregate

During the mixing of concrete or mortar, i.e., before the hydration reaction, a significant amount of water may be taken up by the aggregate. This is the case with oven-dried quartz aggregate, which is the focus of this paper. Accordingly, the total mass of water, w , is decomposed into that of the water in the cement paste, w_{cp} , and that which is absorbed in the open porosity of the quartz, w_a

$$w = w_{cp}(\xi) + w_a(\xi) \quad (1)$$

During the hydration reaction, however, part of the water which has been initially absorbed into the aggregate is sucked back into the interaggregate space, which is then occupied by the cement paste. This is because the hydration products fill less volume than their unreacted counterparts. The volume reduction during cement paste hydration [also called chemical shrinkage (Powers and Brownard 1946; Acker and Ulm 2001; Jensen and Hansen 2001)] leads to the formation of air voids, which are partially refilled by the additional water extracted from the aggregate. This process driven by water supply from the aggregate is sometimes called internal curing (Bentz et al. 2005; Jensen and Lura 2006; Wyrzykowski et al. 2011; Zhutovsky and Kovler 2012; Justs et al. 2015). Maintaining the philosophy of the Powers model to identify linear relations between chemical reactants and products on the one hand and the degree of hydration on the other hand, the authors envision that the amount of aggregate-extracted water increases linearly with the volume of voids. The latter increases linearly with the mass of hydrates formed, which then increases, again linearly, with the degree of hydration. Hence the water content in the cement paste is linearly linked to the hydration degree as well, which is mathematically expressed as follows:

$$\frac{w_{cp}(\xi)}{c} = d + k\xi \quad (2)$$

In this context, $w_{cp}(\xi)$ is the mass of all the water in the cement paste in the most general understanding, i.e., both the unreacted water and that which is chemically combined to the cement clinker; in the same sense, c denotes the total mass of cement, including both the unreacted cement and that which is chemically combined with water. The material constants in Eq. (2), d and k , are the initial value of the water:cement mass ratio which is effective at the cement paste level, and the hydration-dependent (linear) increase of this effective mass ratio, respectively. The former constant can be linked to the water mass which is initially taken up by the aggregate, $w_a(0)$. This quantity is normalized by the mass of the aggregate, a , yielding the initial water:aggregate mass ratio in the form $w_a(0)/a$. When splitting the (nominal) water:cement mass ratio into a cement paste-specific and an aggregate-specific portion, the respective mathematical expression can be readily solved for d , according to

$$\frac{w}{c} = \frac{w_{cp}(0)}{c} + \frac{w_a(0)}{a} \frac{a}{c} \Rightarrow d = \frac{w_{cp}(0)}{c} = (w/c) - \frac{w_a(0)}{a} (a/c) \quad (3)$$

To model the suction of water from the aggregate back to the interaggregate space, which is then occupied by cement paste, cement-specific void-filling extent α between 0 and 1 is introduced, where 0 refers to no water filling the air voids formed during chemical shrinkage of the cement paste and 1 refers to complete filling of the air voids by water. Thereby the voids themselves evolve linearly with the hydration degree (Fig. 1). This void-filling extent α can be related to the back-suction-related parameter k by deriving an expression for the hydration-dependent water mass which was sucked into the cement paste, through combination of Eqs. (2) and (3), yielding

$$w_{cp}(\xi) - w_{cp}(0) = ck\xi \quad (4)$$

and by expressing this mass as the volume of voids multiplied by the void-filling extent α multiplied by the mass density of water, yielding

$$ck\xi = V_{void}\alpha\rho_{H_2O} \quad (5)$$

To relate the void volume V_{void} to the initial composition of the cement paste and to the hydration degree, the void volume is considered to be equal to the volume of cement paste, V_{cp} , multiplied by the cement paste-related volume fraction of voids, f_{void}^{cp}

$$V_{void} = V_{cp}f_{void}^{cp} \quad (6)$$

The volume of cement paste is—in good approximation, i.e., without explicit consideration of autogenous shrinkage—equal to the initial volumes of cement and water, i.e., V_c and V_w , which can be expressed by the masses of cement and water as well as by the related mass densities as

$$V_{cp} = V_c + V_w = \frac{c}{\rho_{clin}} + \frac{w_{cp}(0)}{\rho_{H_2O}} \quad (7)$$

Finally, the volume fraction of shrinkage-induced voids in cement paste is considered to increase proportionally to the hydration degree, as quantified through the Powers-Acker-Hansen hydration model (Powers and Brownard 1946; Acker and Ulm 2001; Jensen and Hansen 2001), evaluated for the effective initial composition of the cement paste matrix, quantified in terms of the effective initial water:cement mass fraction $w_{cp}(0)/c$ [cf. Eq. (15.4) of Pichler et al. (2009)]:

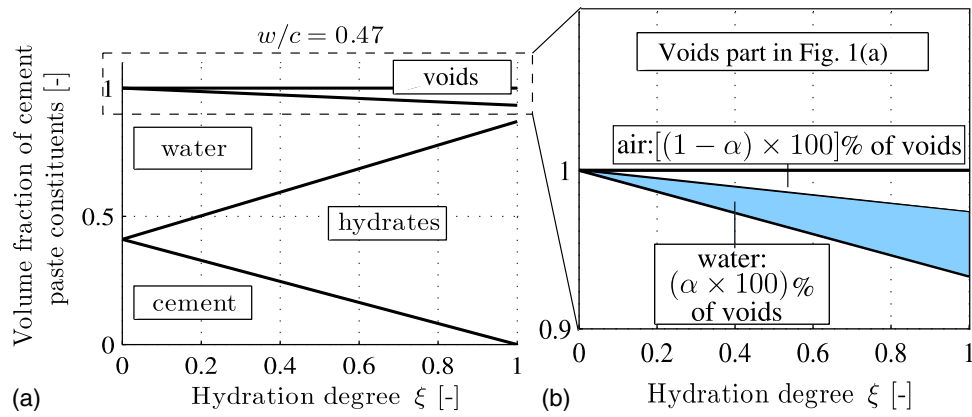


Fig. 1. Hydration-driven evolution of volume fractions of cement paste constituents (cement, water, hydrates, and voids) according to Powers–Acker–Hansen’s hydration model: (a) complete phase volume evolution diagram according to (Powers and Brownyard 1946; Acker and Ulm 2001; Jensen and Hansen 2001); (b) detail illustrating void-filling extent α concerning partial void filling by water that is sucked from the open porosity of quartz into the cement paste matrix

$$f_{void}^{cp} = \frac{(1 + 0.42 \frac{\rho_{clin}}{\rho_{H_2O}} - 1.42 \frac{\rho_{clin}}{\rho_{hyd}})\xi}{1 + \frac{\rho_{clin}}{\rho_{H_2O}}(w_{cp}(0)/c)} = \frac{3.31\xi}{20 + 63 \frac{w_{cp}(0)}{c}} \quad (8)$$

where $\rho_{clin} = 3.150 \text{ kg/dm}^3$ (Acker 2001), $\rho_{H_2O} = 1.000 \text{ kg/dm}^3$, and $\rho_{hyd} = 2.073 \text{ kg/dm}^3$ (Barthélémy and Dormieux 2003) denote the mass densities of cement clinker grains, water, and hydrates, respectively. The relation between the constant k and the void-filling extent of water, α , follows from specialization of Eq. (5) for Eqs. (6)–(8) and solving the resulting expression for k , yielding

$$k = \left[\frac{\rho_{H_2O}}{\rho_{clin}} + \frac{w_{cp}(0)}{c} \right] \frac{3.31\alpha}{20 + 63 \frac{w_{cp}(0)}{c}} \quad (9)$$

Eq. (9) highlights the fact that k , the hydration degree–related rate of the effective water:cement mass fraction of the cement paste matrix [Eq. (2)], is directly proportional to α , the extent to which the shrinkage-induced voids in the cement paste are filled by water.

With respect to the classical Powers–Acker–Hansen model, the hydration model developed herein which also considers internal curing contains two additional quantities: (1) the water uptake capacity of the aggregate, $w_a(0)/a$; and (2) the void-filling extent of water, α . The former quantity is involved in the expression for the initial value of the effective water:cement mass fraction [Eq. (3)], whereas α is involved in the mathematical expression for the evolution of the water:cement mass ratio which is effective in the cement paste, and this expression is obtained by specializing Eq. (2) for d and k according to Eqs. (3) and (9), respectively, and from consideration of the mass densities $\rho_{clin} = 3.150 \text{ kg/dm}^3$ and $\rho_{H_2O} = 1.000 \text{ kg/dm}^3$, as

$$\begin{aligned} \frac{w_{cp}(\xi)}{c} &= (w/c) - \frac{w_a(0)}{a}(a/c) \\ &+ \left[\left(\frac{\rho_{H_2O}}{\rho_{clin}} + \frac{w_{cp}(0)}{c} \right) \frac{3.31\alpha}{20 + 63 \frac{w_{cp}(0)}{c}} \right] \xi \\ &= (w/c) - \frac{w_a(0)}{a}(a/c) \\ &+ \left[\frac{1.051 + 3.31[(w/c) - \frac{w_a(0)}{a}(a/c)]}{20 + 63[(w/c) - \frac{w_a(0)}{a}(a/c)]} \right] \alpha \xi \quad (10) \end{aligned}$$

This is the water:cement mass ratio which is effective at the cement paste level, and which governs the hydration reaction taking place there. Its initial value needs to be considered when quantifying the volume fractions of cement paste and aggregate in a material volume of concrete or mortar with water-absorbing aggregate; except for the use of this effective water:cement mass ratio, the latter quantification follows the standard relation given by Bernard et al. (2003) and Pichler et al. (2009), which yields

$$\begin{aligned} f_{cp}^{no-air} &= \frac{\frac{\rho_{agg}}{\rho_{clin}} + \frac{\rho_{agg}}{\rho_{H_2O}} [w_{cp}(0)/c]}{\frac{\rho_{agg}}{\rho_{clin}} + \frac{\rho_{agg}}{\rho_{H_2O}} [w_{cp}(0)/c] + (a/c)} \\ &= \frac{0.8406 + 2.648[(w/c) - \frac{w_a(0)}{a}(a/c)]}{0.8406 + 2.648[(w/c) - \frac{w_a(0)}{a}(a/c)] + (a/c)} \\ f_{agg}^{no-air} &= \frac{(a/c)}{\frac{\rho_{agg}}{\rho_{clin}} + \frac{\rho_{agg}}{\rho_{H_2O}} [w_{cp}(0)/c] + (a/c)} \\ &= \frac{(a/c)}{0.8406 + 2.648[(w/c) - \frac{w_a(0)}{a}(a/c)] + (a/c)} \quad (11) \end{aligned}$$

where $\rho_{agg} = 2.648 \text{ kg/dm}^3$ is the mass density of quartz aggregate in this paper. However, it often occurs during mixing that small amounts of air are entrapped into the cement paste matrix as well. Denoting the corresponding air volume fraction by f_{air} , the volume fractions at the concrete or mortar level can be derived from the relations

$$f_{cp} + f_{agg} + f_{air} = 1 \quad \frac{f_{cp}}{f_{agg}} = \frac{f_{cp}^{no-air}}{f_{agg}^{no-air}} \quad (12)$$

which imply that

$$f_{cp} = \frac{1 - f_{air}}{1 + f_{agg}^{no-air}/f_{cp}^{no-air}}, \quad f_{agg} = \frac{1 - f_{air}}{1 + f_{cp}^{no-air}/f_{agg}^{no-air}} \quad (13)$$

The relevance of this new water-migration model and its effect on concrete composition were tested through a creep upscaling analysis from the cement paste level to the concrete or mortar level.

Creep Homogenization of Mortars and Concretes

The relevance of the effective water:cement mass ratio according to Eq. (10) and of the cement paste and aggregate volume fractions according to Eqs. (11) and (13), both depending on the void-filling extent α and the water uptake capacity of the aggregate, $w_a(0)/a$, checked by using Eqs. (10), (11), and (13) and the quantities appearing therein within a creep upscaling analysis from the cement paste to the mortar and concrete level.

The purpose of this was to determine whether the experimental results of numerous creep tests performed at the level of cement paste made from *only one* type of cement, and at the level of mortars and concretes made from *the same* type of cement but with two different types of aggregates, can be predicted by a micromechanical model which is based on *only one* value for the cement-specific void-filling capacity α and of *only two* aggregate-specific values for the water-absorption capacity $w_a(0)/a$.

The creep tests considered in this context all followed the protocol reported by Irfan-ul-Hassan et al. (2016). Accordingly, 3-min creep tests on the same cement paste, mortar, or concrete samples were repeated hourly. The key idea behind this protocol is that 3 min is short enough for the microstructure to remain practically *the same* throughout each individual test. Within 1 h, on the other hand, the hydration process in early-age cementitious systems continues in a significant manner, so that two subsequent 3-min creep tests involve remarkably different microstructures. In addition, 3 min is so short and the load levels used are so small that creep strains are—up to the very fine measurement accuracy of the displacement sensors used—fully recovered during the waiting period following each test (Irfan-ul-Hassan et al. 2016). Therefore the individual 3-min tests can be analyzed as independent experiments, i.e., there is no need to consider the entire loading history. Hence an upscaling analysis concerning cement paste, mortar, and concrete samples tested according to the aforementioned protocol can be performed in the theoretical framework of classical, nonaging microviscoelasticity (Read 1950; Sips 1951; Laws and McLaughlin 1978; Beurthey and Zaoui 2000).

Choosing, in this context, a standard micromechanical representation for mortar and concrete (Scheiner and Hellmich 2009; Baweja et al. 1998; Bernard et al. 2003; Hellmich and Mang 2005), namely that of a composite material consisting of a (viscoelastic) cement paste matrix with (elastic) aggregate inclusions and (potentially occurring) air inclusions (Fig. 2) the (homogenized) relaxation tensor at the concrete/mortar scale, \mathbb{R}_{hom} , follows from those at the cement paste scale, \mathbb{R}_{cp} , as well as from the volume

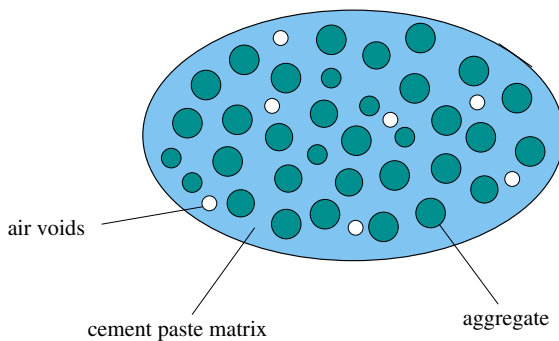


Fig. 2. Micromechanical representation of mortar and concrete: two-dimensional sketch of three-dimensional matrix-inclusion composites composing a continuous cement paste matrix with embedded spherical inclusions representing quartz aggregate and air pores

fractions of cement paste, aggregate, and (potentially occurring) air, as (Scheiner and Hellmich 2009)

$$\begin{aligned} \mathbb{R}_{hom}^*(p) &= 3k_{hom}^*(p)\mathbb{I}_{vol} + 2\mu_{hom}^*(p)\mathbb{I}_{dev} \\ &= (f_{cp}\mathbb{R}_{cp}^* + f_{agg}\mathbb{R}_{agg}^* \cdot \{\mathbb{I} + \mathbb{P}_{sph}^*(p) : [\mathbb{R}_{agg}^* - \mathbb{R}_{cp}^*(p)]\}^{-1}) \\ &\quad + f_{air}\mathbb{R}_{air}^* \cdot \{\mathbb{I} + \mathbb{P}_{sph}^*(p) : [\mathbb{R}_{air}^* - \mathbb{R}_{cp}^*(p)]\}^{-1}) : (f_{cp}\mathbb{I} \\ &\quad + f_{agg}\{\mathbb{I} + \mathbb{P}_{sph}^*(p) : [\mathbb{R}_{agg}^* - \mathbb{R}_{cp}^*(p)]\}^{-1} \\ &\quad + f_{air}\{\mathbb{I} + \mathbb{P}_{sph}^*(p) : [\mathbb{R}_{air}^* - \mathbb{R}_{cp}^*(p)]\}^{-1})^{-1} \end{aligned} \quad (14)$$

where * indicates Laplace–Carson (LC) transforms of the originally time-dependent quantities occurring in the standard convolution integrals of linear viscoelasticity [correspondence principle; (Read 1950; Sips 1951; Laws and McLaughlin 1978; Beurthey and Zaoui 2000)]

$$f^*(p) = p\hat{f}(p) = p \int_0^\infty f(t) \exp(-pt) dt \quad (15)$$

and back-transformation of Eq. (14) from the Laplace–Carson domain to the time domain may be performed by the Gaver–Wynn–Rho algorithm (Scheiner and Hellmich 2009; Gaver 1966). The Appendix provides mathematical details of the LC-transformed homogenized bulk and shear moduli, k_{hom}^* and μ_{hom}^* ; the fourth-order unity tensor \mathbb{I} with its volumetric and deviatoric parts, \mathbb{I}_{vol} and \mathbb{I}_{dev} ; and the morphology tensor \mathbb{P}_{sph}^* . The relaxation tensors \mathbb{R}_{cp}^* correspond to a power law-type creep behavior characterized by an elastic modulus E_{cp} , a Poisson's ratio ν_{cp} , a creep modulus $E_{c,cp}$, and a creep exponent β_{cp}

$$\begin{aligned} \mathbb{R}_{cp}^*(p) &= 3k_{cp}^*(p)\mathbb{I}_{vol} + 2\mu_{cp}^*(p)\mathbb{I}_{dev} \\ &= \left[\frac{1-2\nu_{cp}}{E_{cp}} + \frac{1-2\nu_{cp}}{E_{c,cp}} \left(\frac{1}{t_{ref}} \right)^{\beta_{cp}} \Gamma(\beta_{cp} + 1) p^{-\beta_{cp}} \right]^{-1} \mathbb{I}_{vol} \\ &\quad + \left[\frac{1+\nu_{cp}}{E_{cp}} + \frac{1+\nu_{cp}}{E_{c,cp}} \left(\frac{1}{t_{ref}} \right)^{\beta_{cp}} \Gamma(\beta_{cp} + 1) p^{-\beta_{cp}} \right]^{-1} \mathbb{I}_{dev} \end{aligned} \quad (16)$$

The aforementioned material characteristics at the cement-paste level all depend on the (here, effective) water:cement mass ratio and the hydration degree, as identified in the more than 500 creep tests on cement paste reported by Irfan-ul-Hassan et al. (2016) (Fig. 3). Quadratic interpolation between experimental data was used to consider the (effective) water:cement mass ratios between those which were explicitly tested (Fig. 4). This allow for remaining as close as possible to the measured properties, thereby avoiding the (small) uncertainties resulting from the application of available multiscale models. However, this was not possible for the quantification of Poisson's ratio, which was not measured experimentally. Therefore a validated multiscale model (Pichler et al. 2008; Pichler and Hellmich 2011) was used to establish a relationship between the Poisson's ratio and the elastic modulus (Fig. 5).

This study is devoted to aggregate consisting of quartz, with elastic bulk and shear moduli of Bass (2013)

$$\begin{aligned} k_{agg} &= 37.8 \text{ GPa}, \\ \mu_{agg} &= 44.3 \text{ GPa} \Rightarrow \mathbb{R}_{agg}^* = 3k_{agg}\mathbb{I}_{vol} + 2\mu_{agg}\mathbb{I}_{dev} \end{aligned} \quad (17)$$

Air inclusions, if they exist, do not exhibit a solid elastic stiffness

$$k_{air} = \mu_{air} = 0 \text{ GPa}, \Rightarrow \mathbb{R}_{air}^* = 0 \quad (18)$$

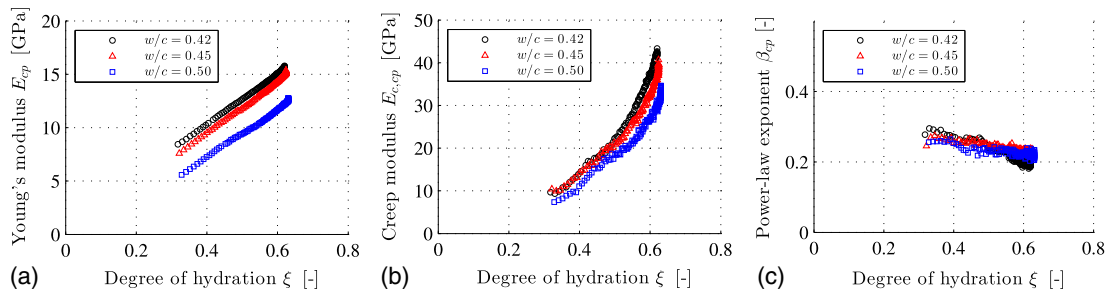


Fig. 3. Results from hourly-repeated 3-min creep testing on cement pastes with initial water:cement mass ratios of 0.42, 0.45, and 0.50, as functions of hydration degree (data from Irfan-ul-Hassan et al. 2016): (a) elastic modulus E_{cp} ; (b) creep modulus $E_{c,cp}$; (c) creep exponent β_{cp}

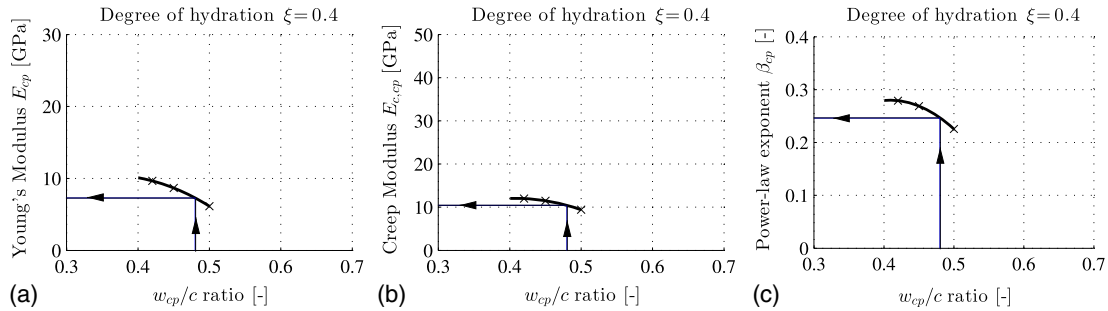


Fig. 4. Quantification of effective viscoelastic properties of cement paste matrix as a function of effective water:cement mass fraction w_{cp}/c by means of quadratic interpolation between creep test results on plain cement pastes with $w/c \in [0.42, 0.45, 0.50]$ at degree of hydration $\xi = 0.40$: (a) elastic modulus E_{cp} ; (b) creep modulus $E_{c,cp}$; (c) creep exponent β_{cp}

Comparison of Ultrashort Creep Experiments and Corresponding Micromechanics Predictions: Identification of Water Absorption Capacities of Quartz Aggregate and of Paste Void-Filling Extent

Experimental Campaign on Mortar/Concrete Level

In order to assess the relevance of the newly introduced quantities, the paste void-filling extent α and the water-absorption capacity of aggregate, $w_a(0)/a$, expressed in corresponding creep homogenization results described in the previous section, the latter results need to be compared with experimental data at the level of mortar

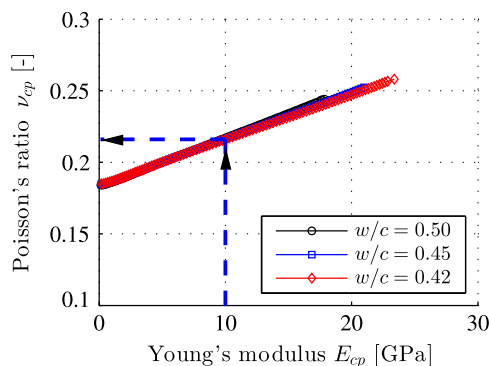


Fig. 5. Relation between elastic modulus and Poisson's ratio of cement pastes with initial water:cement mass ratios of 0.42, 0.45, and 0.50; predictions of the validated multiscale model of Pichler et al. (2009) and Pichler and Hellmich (2011)

and concrete. To this end, a series of 3-min creep tests on two mortars and two concretes was performed.

All four materials exhibited the same nominal volume fractions of quartz aggregate and of cement paste, 0.58 and to 0.42, respectively (Table 1). Mortar #1 and Concrete #1 exhibited the same nominal composition in terms of $w/c = 0.50$ and $a/c = 3.0$. Mortar #2 and Concrete #2 exhibited $w/c = 0.42$ and $a/c = 2.7$. All four materials were produced from a commercial cement of type CEM I 42.5 N and distilled water, i.e., with the same raw materials that were also used for the production of the cement pastes discussed by Irfan-ul-Hassan et al. (2016). In addition, oven-dried aggregate made of quartz was used. The two mortars contained standard sand from Normensand (Beckum, Germany) consisting of rounded quartz grains with maximum diameter $d_{max} = 2$ mm. The two concretes contained aggregate from Pannonia Kies (Wien, Austria), consisting of quartz gravel with maximum diameter $d_{max} = 8$ mm.

The early-age testing protocol was identical to that used to characterize cement paste [see Irfan-ul-Hassan et al. (2016)], i.e., the mortar and concrete specimens with dimensions 70 mm diameter and 300 mm height were hourly subjected to 3-min creep tests under uniaxial stress conditions [Fig. 6(a)]. For each test, the load

Table 1. Nominal Composition of Tested Mortars and Concretes

Material	w/c	a/c	f_{cp}^{nom}	f_{agg}^{nom}	d_{max} (mm)
Mortar #1	0.50	3.0	0.42	0.58	2
Mortar #2	0.42	2.7	0.42	0.58	2
Concrete #1	0.50	3.0	0.42	0.58	8
Concrete #2	0.42	2.7	0.42	0.58	8

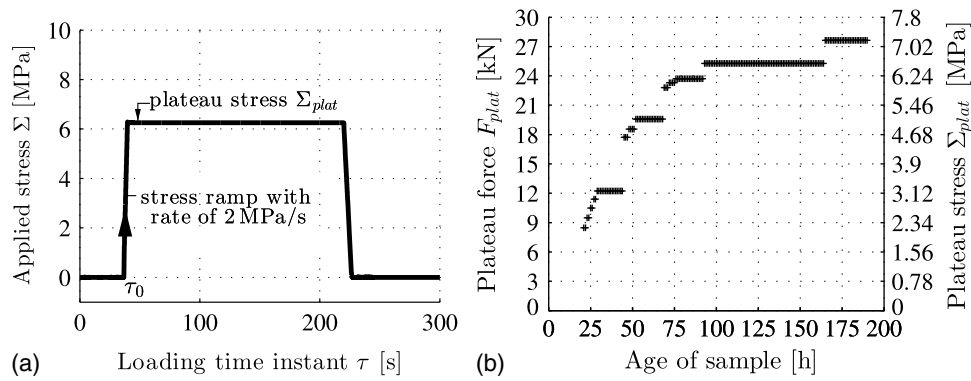


Fig. 6. Three-min creep tests on mortars and concretes: (a) force history during creep testing carried out at an age of 100 h on Mortar #1; (b) prescribed load levels chosen to be less than or equal to 15% of the expected compressive strength

plateau was selected so that induced compressive stresses were less than 15% of the expected compressive strength [Fig. 6(b)]. Using the calorimetry results described by Irfan-ul-Hassan et al. (2016), sample ages were translated into equivalent hydration degrees.

Each specimen was subjected to 168 individual 3-min creep tests. Out of this database, focus was placed on the tests carried out at the following hydration degrees:

$$\xi \in [0.32, 0.35, 0.40, 0.45, 0.50, 0.55, 0.60, 0.63] \quad (19)$$

The plateau stresses (Fig. 6) which correspond to the hydration degrees of Eq. (19) were

$$\Sigma_{plat} = [2.08, 2.32, 3.0, 3.0, 4.37, 4.83, 6.25, 6.25] \text{ MPa} \quad (20)$$

The corresponding normal strains in loading direction, $E(t)$, were divided by the applied plateau stress Σ_{plat} (Fig. 6) to arrive at a convenient illustration of the test results (Fig. 7).

Micromechanical Predictions of Experimental Data

To micromechanically predict the creep test results (Fig. 7), the relaxation functions of Eq. (14) were transformed to creep functions according to

$$\begin{aligned} \mathbb{J}_{hom}^*(p) &= \mathbb{R}_{hom}^*(p)^{-1} \\ \mathbf{E}^*(p) &= \mathbb{J}_{hom}^*(p) : \boldsymbol{\Sigma}^*(p) \end{aligned} \quad (21)$$

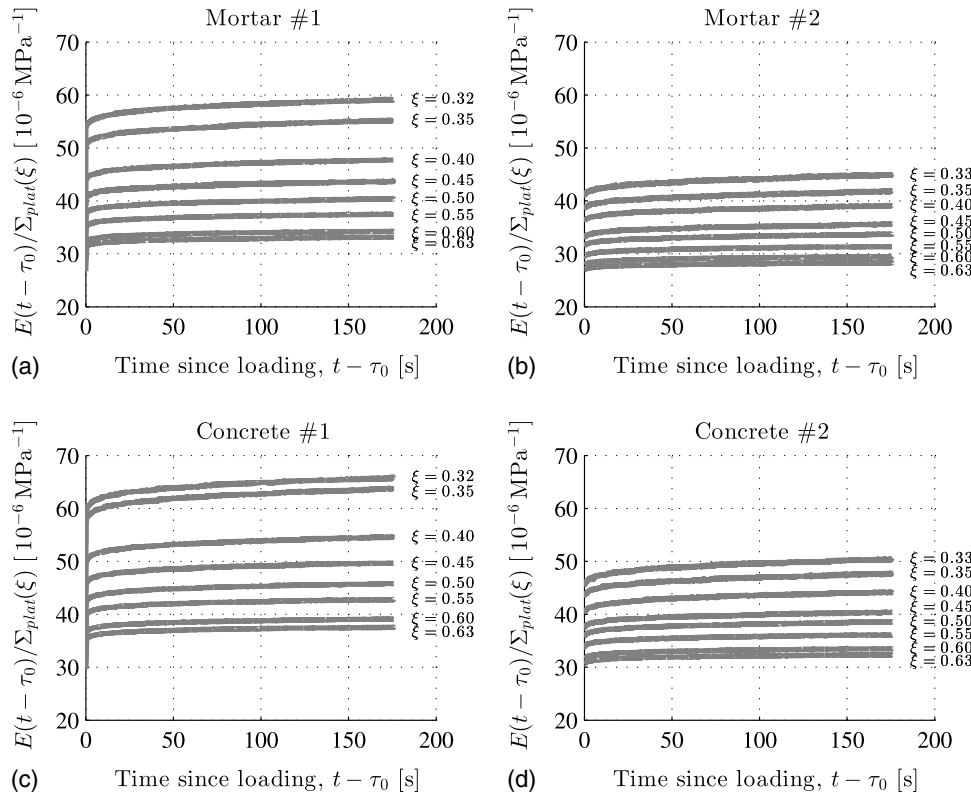


Fig. 7. Plateau stress–normalized strains obtained from 3-min creep tests on mortars and concretes at the hydration degrees according to Eq. (19), for the corresponding load plateaus see Eq. (20): (a) Mortar #1: $w/c = 0.50$, $a/c = 3.00$; (b) Mortar #2: $w/c = 0.42$, $a/c = 2.70$; (c) Concrete #1: $w/c = 0.50$, $a/c = 3.00$; (d) Concrete #2: $w/c = 0.42$, $a/c = 2.70$

Table 2. Prediction Errors \mathcal{E} (MPa⁻¹) according to Eq. (24)

Material	\mathcal{E} with nominal composition	\mathcal{E} obtained with water-migration model
Mortar #1	4.50×10^{-6}	1.55×10^{-7}
Mortar #2	1.50×10^{-6}	2.90×10^{-7}
Concrete #1	5.50×10^{-6}	1.50×10^{-7}
Concrete #2	1.23×10^{-6}	1.30×10^{-7}

and these results were then back-transformed into the time domain, yielding

$$E(\xi, t) = \int_0^t J_{hom}(\xi, t - \tau) : \dot{\Sigma}(\tau) d\tau \quad (22)$$

This Boltzmann convolution integral was then evaluated for the volume fractions of Eqs. (11) and (13), for the cement paste properties of Fig. 4, and for the loading history of Fig. 6. These evaluations comprised two quantities which were not known a priori, but which were identified from a series of creep results at the concrete and mortar levels. This is described in the following sections.

Furthermore, consideration of the load history of Fig. 6 as a continuous function, rather than as a step function, and corresponding use of the continuous form of the Boltzmann integral [Eq. (22)] is mandatory for arriving at reliable results. This is because a ramp loading as indicated in Fig. 6 provokes not only elastic but also viscoelastic strains (Irfan-ul-Hassan et al. 2016).

Identification of Water Uptake Capacity of Normensand Quartz Aggregate and of the Paste Void-Filling Extent from Experimental Data of Mortar #1

The water uptake capacity of quartz, $w_a(0)/a$, and the paste void-filling extent, α , were identified from a very large set of numerical values making up the following search intervals:

$$w_a(0)/a \in [0.000, 0.0001, 0.0002, \dots, 0.0199, 0.0200]$$

$$\alpha \in [0.000, 0.001, 0.002, \dots, 0.999, 1.000] \quad (23)$$

For all data pairs $[w_a(0)/a, \alpha]$ composed from the values in Eq. (23), the micromechanics model of Eqs. (14)–(18), together with Eqs. (3), (10), and (11) evaluated for $w/c = 0.50$ and $a/c = 3.0$ (Table 1), with the interpolation scheme of Fig. 4 and with the

loading history of Fig. 6 applied to Eq. (22), were used to predict the creep functions arising from the eight creep tests conducted on Mortar #1 [Fig. 7(a)]. Eight hydration degree-specific model predictions of the normal strain histories E^{pred} , represented by 180 discrete values each, were compared with the corresponding experimentally determined strains normalized by plateau stress E^{exp} , and the corresponding prediction error was quantified through

$$\mathcal{E} = \frac{1}{8 \times 180} \sum_{i=1}^8 \frac{1}{\Sigma_{plat}(\xi_i)} \sum_{j=1}^{180} |E^{pred}(\xi_i, t_j) - E^{exp}(\xi_i, t_j)| \quad (24)$$

whereby all strain values were normalized with respect to the plateau stresses Σ_{plat} . The smallest prediction error $\mathcal{E} = 1.55 \times 10^{-7}$ MPa⁻¹ (Table 2) was obtained for the following values of the water uptake capacity of quartz and of the water-filling extent of shrinkage-induced voids:

$$\frac{w_a(0)}{a} = 0.0099 \quad \alpha = 0.603 \quad (25)$$

Fig. 8(a) compares the measured and the modeled creep functions. The material constants in Eq. (25) imply that 1 kg quartz takes up 9.9 g water during mixing of the raw materials, and that shrinkage-induced voids of the cement paste matrix suck back water from the open porosity of quartz such that these voids are water-filled to an extent of 60.3%.

The identified material constants in Eq. (25) provide access to the effective composition of the cement paste of Mortar #1. The initial value of the effective water:cement mass fraction of the cement paste matrix, for instance, follows from specialization of Eq. (3) for the value of $w_a(0)/a$ in Eq. (25) and for the mix-related water:cement and quartz:cement mass ratios $w/c = 0.50$ and $a/c = 3.0$ as

$$\frac{w_{cp}(0)}{c} = 0.4703 \quad (26)$$

This is remarkably smaller than the (nominal) mix-related water:cement mass ratio $w/c = 0.50$. The evolution of the effective water:cement mass fraction of the cement paste matrix follows from specialization of Eq. (10) for Eq. (25), $w/c = 0.50$, and $a/c = 3.0$ as [Fig. 8(b)]

$$\frac{w_{cp}(\xi)}{c} = 0.4703 + 0.0317\xi \quad (27)$$

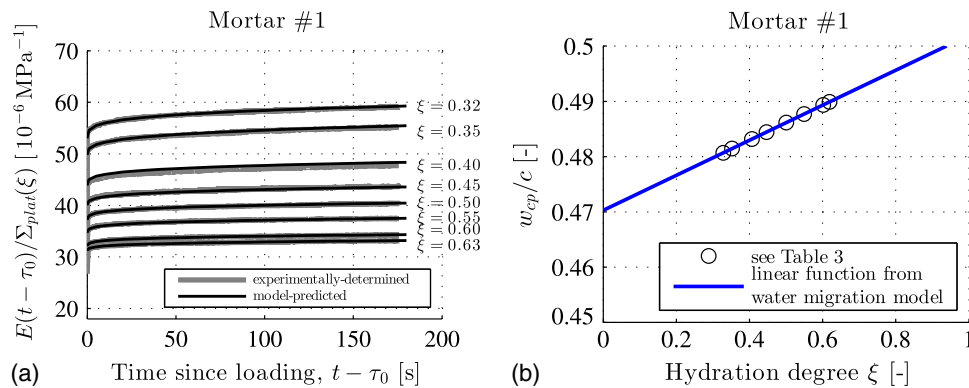


Fig. 8. Application of water-migration model according to Eq. (10) to Mortar #1 with mix-related (nominal) composition given through $w/c = 0.50$ and $a/c = 3.0$, and water uptake capacity of quartz and void water-filling extent according to Eq. (25): (a) comparison of experimentally determined and model-predicted plateau stress-normalized strains at hydration degrees according to Eq. (19), for the corresponding load plateaus see Eq. (20); (b) evolution of effective water:cement mass fraction of cement paste matrix as a function of degree of hydration; for the complete set of material properties of cement paste, see Table 3

Table 3. Input Quantities for Creep Homogenization of Mortar #1 (Table 1): Effective Water:Cement Mass Ratios of the Cement Paste Matrix according to Eqs. (10) and (25) and Its Viscoelastic Properties Found by Interpolation (Fig. 4)

ξ	$w_{cp}(\xi)/c$	E_{cp} (GPa)	ν_{cp}	$E_{c,cp}$ (GPa)	β_{cp}
0.32	0.480	6.529	0.205	9.218	0.269
0.35	0.481	7.041	0.206	8.562	0.267
0.40	0.483	8.223	0.210	13.220	0.242
0.45	0.484	9.172	0.214	15.775	0.228
0.50	0.486	10.236	0.217	19.270	0.219
0.55	0.487	11.274	0.221	23.640	0.210
0.60	0.489	12.442	0.225	29.012	0.209
0.63	0.490	12.843	0.226	30.774	0.208

The actual volume fractions of the cement paste matrix and of quartz follow from specialization of Eq. (11) for Eq. (26), $w/c = 0.50$, and $a/c = 3.0$ as

$$f_{cp} = 0.4101, \quad f_{agg} = 0.5899 \quad (28)$$

Confirmation of Water Uptake Capacity of Normensand Quartz Aggregate and of the Paste Void-Filling Extent through Experimental Data of Mortar #2

Because Mortars #1 and #2 were produced with the same raw materials, the material constants in Eq. (25) are not only valid for Mortar #1, but they must also hold for Mortar #2, i.e., the strain evolutions measured during creep testing of Mortar #2 must be predictable, and this was checked next. To this end, the initial value of the effective water:cement mass fraction of the cement paste matrix follows from specialization of Eq. (3) for $w_a(0)/a$ from Eq. (25) and for the mix-related water:cement and quartz:cement mass ratios $w/c = 0.42$ and $a/c = 2.7$ as

$$\frac{w_{cp}(0)}{c} = 0.3933 \quad (29)$$

This is significantly smaller than the mix-related water:cement mass ratio $w/c = 0.42$. The evolution of the effective water:cement mass fraction of the cement paste matrix follows from specialization of Eq. (10) for Eq. (25), $w/c = 0.42$, and $a/c = 2.7$ as [Fig. 9(b)]

Table 4. Input Quantities for Creep Homogenization of Mortar #2 (Table 1): Effective Water:Cement Mass Ratios of the Cement Paste Matrix according to Eqs. (10) and (25) and Its Viscoelastic Properties Found by Interpolation (Fig. 4)

ξ	$w_{cp}(\xi)/c$	E_{cp} (GPa)	ν_{cp}	$E_{c,cp}$ (GPa)	β_{cp}
0.32	0.403	8.623	0.211	9.719	0.322
0.35	0.404	9.864	0.215	11.857	0.290
0.40	0.405	10.693	0.218	14.872	0.270
0.45	0.407	12.175	0.222	19.312	0.260
0.50	0.409	13.189	0.225	23.055	0.244
0.55	0.410	14.369	0.229	30.780	0.222
0.60	0.412	15.417	0.232	38.460	0.196
0.62	0.413	16.146	0.234	44.927	0.192

$$\frac{w_{cp}(\xi)}{c} = 0.3933 + 0.0317\xi \quad (30)$$

The actual volume fractions of the cement paste matrix and of quartz follow from specialization of Eq. (11) for Eq. (29), $w/c = 0.42$, and $a/c = 2.7$ as

$$f_{cp} = 0.4107, \quad f_{agg} = 0.5893 \quad (31)$$

Viscoelastic properties of the cement paste matrix—valid for effective water:cement mass fractions from Eq. (30), evaluated for all hydration degrees of interest given in Eq. (19)—were quantified by means of interpolation, as described in the previous subsection (Fig. 4).

Model-predicted creep functions for Mortar #2 agreed well with measured creep functions, as quantified by prediction error $\mathcal{E} = 2.90 \times 10^{-7} \text{ MPa}^{-1}$ (Table 2) evaluated according to Eq. (24) [Fig. 9(a)]. This shows not only the satisfactory predictive capabilities of the developed water migration model [Eq. (10)], but also the significance of the identified values of the water uptake capacity of quartz and of the water-filling extent of shrinkage-induced voids [Eq. (25)].

Identification of Water Uptake Capacity of Pannonia Kies Aggregate and of Entrapped Air Content from Experimental Data of Concrete #1

Regarding model prediction of the creep strain evolutions measured in 3-min creep tests on Concrete #1, both concretes were

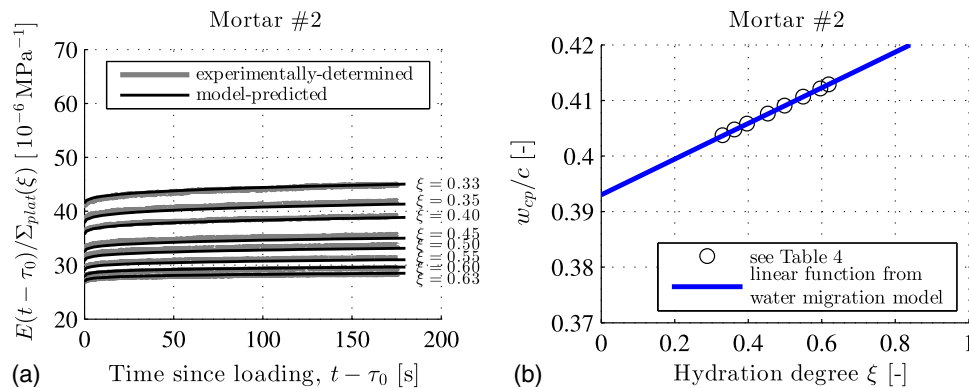


Fig. 9. Application of water-migration model according to Eq. (10) to Mortar #2 with mix-related (nominal) composition given through $w/c = 0.42$ and $a/c = 2.7$ and water uptake capacity of quartz and void water-filling extent according to Eq. (25): (a) comparison of experimentally determined and model-predicted plateau stress-normalized strains at hydration degrees according to Eq. (19), for the corresponding load plateaus see Eq. (20); (b) evolution of effective water:cement mass fraction of cement paste matrix as a function of degree of hydration; for the complete set of material properties of cement paste, see Table 4

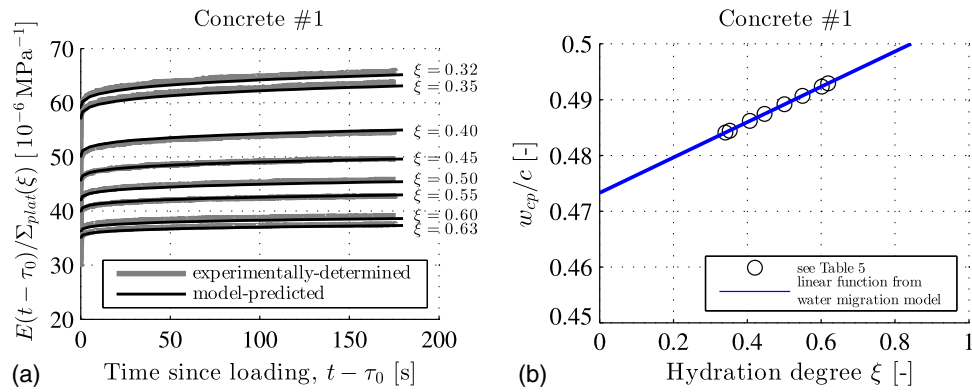


Fig. 10. Application of water-migration model according to Eq. (10) to Concrete #1 with mix-related (nominal) composition given through $w/c = 0.50$ and $a/c = 3.0$, void water-filling extent according to Eq. (25), and water uptake capacity of quartz and entrapped air volume fraction according to Eq. (33): (a) comparison of experimentally determined and model-predicted plateau stress-normalized strains at hydration degrees according to Eq. (19), for the corresponding load plateaus see Eq. (20); (b) evolution of effective water:cement mass fraction of cement paste matrix as a function of degree of hydration; for the complete set of material properties of cement paste, see Table 5

Table 5. Input Quantities for Creep Homogenization of Concrete #1 (Table 1): Effective Water:Cement Mass Ratios of the Cement Paste Matrix according to Eqs. (10) and (25) and Its Viscoelastic Properties Found by Interpolation (Fig. 4)

ξ	$w_{cp}(\xi)/c$	E_{cp} (GPa)	ν_{cp}	$E_{c,cp}$ (GPa)	β_{cp}
0.33	0.484	6.720	0.205	9.096	0.262
0.35	0.4845	6.927	0.206	9.531	0.257
0.40	0.486	7.966	0.210	12.332	0.244
0.44	0.487	8.900	0.213	15.582	0.240
0.50	0.489	9.940	0.216	18.548	0.232
0.55	0.490	10.884	0.219	21.911	0.227
0.60	0.492	12.115	0.224	27.777	0.215
0.63	0.493	12.569	0.225	30.116	0.218

produced with quartz gravel from Pannonia Kies; the corresponding water uptake capacity was unknown and needed to be identified. Notably, this was not sufficient to obtain satisfactory agreement between model-predicted and measured creep functions, because the model-predicted creep functions underestimated the measured creep functions, particularly because the elastic stiffness was overestimated. Therefore the air mixed into the concrete during production was considered. Because all eight creep tests were carried out on the same specimen, just one entrapped air content [Eq. (13)] needed to be identified.

Similar to the identification process described for Mortar #1, the water uptake capacity of the Pannonia Kies quartz and the entrapped air content were identified from the following search intervals:

$$w_a(0)/a \in [0.000, 0.0001, 0.0002, \dots, 0.0199, 0.0200]$$

$$f_{air} \in [0.000, 0.001, 0.002, \dots, 0.049, 0.050] \quad (32)$$

The identified void-filling extent α according to Eq. (25), was considered to be applicable to both concretes.

Accordingly, for all data pairs $[w_a/a(0), f_{air}]$ composed from the values given in Eq. (32), the micromechanics model of Eqs. (14)–(18), together with Eqs. (3), (10), and (11) evaluated for $\alpha = 0.603$, $w/c = 0.50$, and $a/c = 3.0$ (Table 1), with the interpolation scheme of Fig. 4 and with the loading history of Fig. 6 applied to Eq. (22), was used to predict the creep functions arising from the eight creep tests conducted on Concrete #1 [Fig. 7(c)]. Model-predicted creep functions were compared with measured

creep functions, and model prediction errors were quantified according to Eq. (24). The smallest prediction error amounted to $\mathcal{E} = 1.5 \times 10^{-7} \text{ MPa}^{-1}$ (Table 2), and the corresponding values of the water uptake capacity and of the air volume fraction were

$$\frac{w_a(0)}{a} = 0.0089 \quad f_{air} = 0.026 \quad (33)$$

Fig. 10(a) compares the measured and the model-predicted creep functions. The water uptake capacity in Eq. (33) implies that 1 kg Pannonia Kies quartz takes up 8.9 g water during mixing of the raw materials. The corresponding initial value of the effective water:cement mass fraction of the cement paste matrix follows from specialization of Eq. (3) for the value of $w_a(0)/a$ from Eq. (33) and for the mix-related water:cement and quartz:cement mass ratios $w/c = 0.50$ and $a/c = 3.0$ as

$$\frac{w_{cp}(0)}{c} = 0.4733 \quad (34)$$

This is significantly smaller than the mix-related water:cement mass ratio $w/c = 0.50$. The evolution of the effective water:cement mass fraction of the cement paste matrix follows from specialization of Eq. (10) for α from Eq. (25), $w_a(0)/a$ from Eq. (33), $w/c = 0.50$, and $a/c = 3.0$, as [Fig. 10(b)]

$$\frac{w_{cp}(\xi)}{c} = 0.4733 + 0.0317\xi \quad (35)$$

The actual volume fractions of the cement paste matrix and of quartz follow from Eqs. (33) and (34), $w/c = 0.50$, $a/c = 3.0$, and Eqs. (11) and (13) as

$$f_{cp} = 0.4004, \quad f_{agg} = 0.5736 \quad (36)$$

The satisfactory agreement between the model-predicted and measured creep functions further corroborates the developed water-migration model [Eq. (10)] and the void water-filling extent α given in Eq. (25).

Confirmation of Water Uptake Capacity of Pannonia Kies Aggregate through Experimental Data of Concrete #2

Because Concretes #1 and #2 were produced with the same quartz gravel, the water uptake capacity was already known [Eq. (33)].

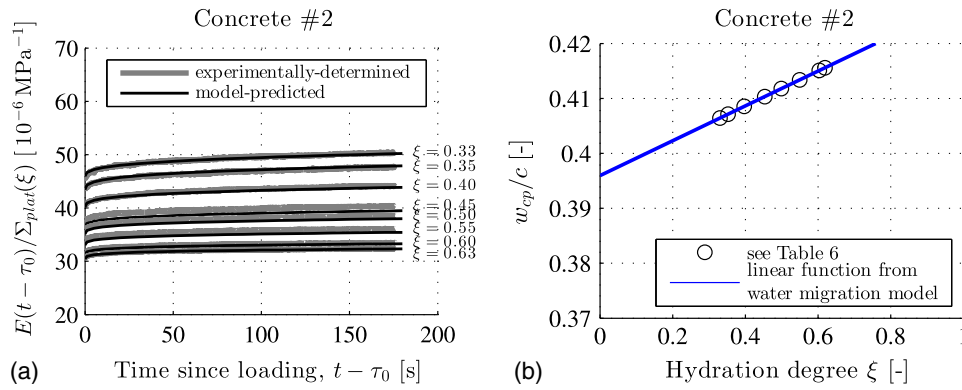


Fig. 11. Application of the water migration model according to Eq. (10) to Concrete #2, with a mix-related (nominal) composition given through $w/c = 0.42$ and $a/c = 2.7$, with void water-filling extent according to Eq. (25), with water uptake capacity of quartz according to Eqs. (33) and with entrapped air volume fraction according to Eq. (37): (a) comparison of experimentally-determined and model-predicted plateau stress-normalized strains, at the hydration degrees according to Eq. (19), for the corresponding load plateaus see Eq. (20); (b) evolution of effective water:cement mass fraction of the cement paste matrix, as a function of degree of hydration; for the complete set of material properties of cement paste, see Table 6

Table 6. Input Quantities for Creep Homogenization of Concrete #2 (Table 1): Effective Water:Cement Mass Ratios of the Cement Paste Matrix according to Eqs. (10) and (25) and Its Viscoelastic Properties Found by Interpolation (Fig. 4)

ξ	$w_{cp}(\xi)/c$	E_{cp} (GPa)	ν_{cp}	$E_{c,cp}$ (GPa)	β_{cp}
0.33	0.406	8.519	0.211	9.597	0.312
0.35	0.407	9.268	0.213	10.701	0.286
0.40	0.408	10.477	0.217	14.669	0.265
0.45	0.410	11.921	0.221	19.020	0.255
0.50	0.411	12.791	0.224	22.434	0.238
0.55	0.413	13.940	0.228	29.692	0.218
0.60	0.415	15.153	0.231	38.407	0.195
0.62	0.415	15.672	0.233	43.084	0.191

Furthermore, the void water-filling ratio α was already identified [Eq. (25)]. However, Concrete #2 was tested with a specific specimen, and the related air volume fraction needed to be identified. By analogy to the previously described identification processes, the entrapped air volume fraction was

$$f_{air} = 0.027 \quad (37)$$

The initial value of the effective water:cement mass fraction of the cement paste matrix follows from specialization of Eq. (3) for the value of $w_a(0)/a$ from Eq. (33) and for the mix-related water:cement and quartz:cement mass ratios $w/c = 0.42$ and $a/c = 2.7$ as

$$\frac{w_{cp}(0)}{c} = 0.3960 \quad (38)$$

This is significantly smaller than the mix-related water:cement mass ratio $w/c = 0.42$. The evolution of the effective water:cement mass fraction of the cement paste matrix follows from specialization of Eq. (10) for the value of α from Eq. (25), the value of $w_a(0)/a$ from Eq. (33), $w/c = 0.42$, and $a/c = 2.7$, as [Fig. 11(b)]

$$\frac{w_{cp}(\xi)}{c} = 0.3960 + 0.0317\xi \quad (39)$$

The actual volume fractions of the cement paste matrix and of quartz follow from Eqs. (33) and (38), $w/c = 0.42$, $a/c = 2.7$, and Eqs. (11) and (13) as

$$f_{cp} = 0.4005, \quad f_{agg} = 0.5725 \quad (40)$$

The satisfactory agreement between the model-predicted and measured creep functions, as quantified by prediction error $\mathcal{E} = 1.30 \times 10^{-7} \text{ MPa}^{-1}$ (Table 2), further corroborates the developed water-migration model [Eq. (10)] evaluated for the void water-filling extent α in Eq. (25), and the water uptake capacity $w_a(0)/a$ in Eq. (33).

Discussion

This paper extended the Powers–Acker–Hansen hydration model to consider water migration including (1) the initial water uptake by the aggregate and (2) back-suction of this water to the cement paste matrix during hydration. The following discussion refers to phase volume evolutions predicted by the extended hydration model, to the self desiccation–driven desaturation of cement pastes with and without water migration, and to the driving force for water migration from the aggregate to the cement paste matrix. The section closes with a future outlook.

Cement Paste-Related Phase Volume Evolutions Considering Water Migration

Phase volume diagrams require expressions of phase volumes as functions of the initial water:cement mass ratio $w_{cp}(0)/c$ and the hydration degree ξ . Eq. (8) provides such an expression for shrinkage-induced voids. Similar expressions for cement clinker, water-filled capillary porosity, and gel-porous hydration products are (e.g., Pichler et al. 2009)

$$f_{clin}^{cp} = \frac{1 - \xi}{1 + \frac{\rho_{clin} w_{cp}(0)}{\rho_{H_2O} c}} = \frac{20(1 - \xi)}{20 + 63 \frac{w_{cp}(0)}{c}} \geq 0 \quad (41)$$

$$f_{cap}^{cp} = \frac{\frac{\rho_{clin}}{\rho_{H_2O}} \left[\frac{w_{cp}(0)}{c} - 0.42\xi \right]}{1 + \frac{\rho_{clin} w_{cp}(0)}{\rho_{H_2O} c}} = \frac{63 \left[\frac{w_{cp}(0)}{c} - 0.42\xi \right]}{20 + 63 \frac{w_{cp}(0)}{c}} \geq 0 \quad (42)$$

$$f_{hyd}^{cp} = \frac{1.42 \frac{\rho_{clin}}{\rho_{hyd}} \xi}{1 + \frac{\rho_{clin} w_{cp}(0)}{\rho_{H_2O} c}} = \frac{43.15\xi}{20 + 63 \frac{w_{cp}(0)}{c}} \quad (43)$$

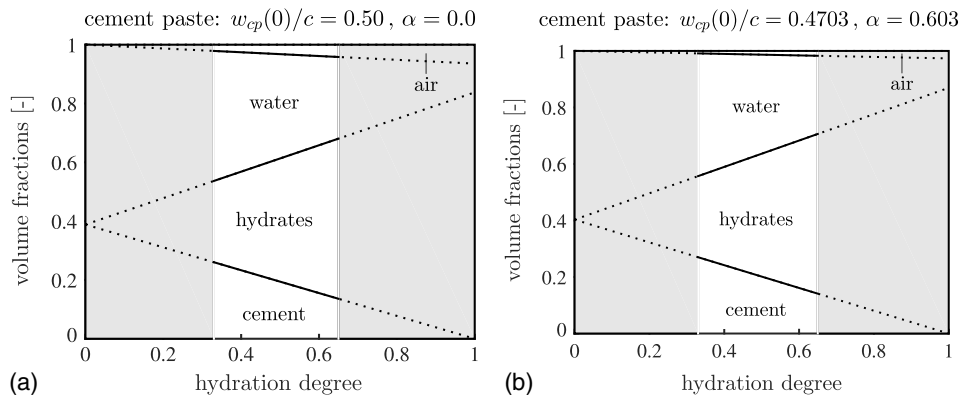


Fig. 12. Phase volume evolutions of cement paste: (a) Powers–Acker–Hansen hydration model for $w/c = 0.50$ (equivalent to inputs $w_{cp}(0)/c = 0.50$ and $\alpha = 0$); (b) proposed water-migration model for cement paste matrix of Mortar #1 with $w_{cp}(0)/c = 0.4703$ and $\alpha = 0.603$; the central nonshaded domain refers to the experimentally investigated interval of hydration degrees $\xi \in [0.32, 0.65]$

To illustrate phase volume evolution diagrams referring to clinker, hydrates, water, and air, it was considered that capillary pores are water saturated, that voids are filled to an extent α by water which is sucked back from the aggregate into the cement paste matrix, and that only the remaining voids are filled by air

$$f_{water}^{cp} = f_{cap}^{cp} + \alpha f_{void}^{cp} \quad (44)$$

$$f_{air}^{cp} = (1 - \alpha) f_{void}^{cp} \quad (45)$$

The effect of water migration on the cement paste matrix of Mortar #1 was studied based on the phase volume expressions Eqs. (8) and (41)–(45). Evaluating those expressions for $w_{cp}(0)/c = 0.50$ and $\alpha = 0$ delivers classical phase volume evolutions of the Powers–Acker–Hansen model [Fig. 12(a)]. Evaluating those expressions for $w_{cp}(0)/c = 0.4703$ and $\alpha = 0.603$ delivers water migration–based phase volume evolutions [Fig. 12(b)]. Comparison of Figs. 12(a and b) shows that the main difference between the two phase volume evolution diagrams concerns the air volume fraction. The latter is significantly smaller in the case of water migration.

Self Desiccation–Driven Desaturation of Cement Paste

The hydration-driven water migration from the aggregate back to the cement paste matrix counteracts to a certain extent the self desiccation–driven desaturation of cement paste. The related saturation ratio is defined as the ratio of water-filled porosity to the total porosity. The latter includes the gel pores. Notably, gel-porous hydration products (labeled hydrates in Fig. 12) include a gel porosity of 28% (Jensen and Hansen 2001), i.e.

$$f_{gel}^{cp} = 0.28 f_{hyd}^{cp} \quad (46)$$

Therefore the total porosity consists of shrinkage-induced voids, capillary pores, and gel pores

$$f_{pores}^{cp} = f_{void}^{cp} + f_{cap}^{cp} + f_{gel}^{cp} \quad (47)$$

and the water-filled porosity is

$$f_{H_2O}^{cp} = \alpha f_{void}^{cp} + f_{cap}^{cp} + f_{gel}^{cp} \quad (48)$$

The saturation ratio follows from combination of Eqs. (42)–(44) and (46)–(48) as

$$S_r = \frac{f_{H_2O}^{cp}}{f_{pores}^{cp}} = \frac{(3.31\alpha - 14.378)\xi + 63 \frac{w_{cp}(0)}{c}}{-11.068\xi + 63 \frac{w_{cp}(0)}{c}} \quad (49)$$

Eq. (49) shows that (1) the saturation ratio superlinearly decreases with increasing hydration degree, and (2) a water-filling extent $\alpha = 0.603$ reduces the self desiccation–related desaturation by almost 60% (Fig. 13).

Back-Suction of Water from Aggregate into Cement Paste Matrix

For the application of the creep homogenization model, it was assumed that the back-sucked water was—in good approximation—uniformly distributed in the cement paste matrix. This is reasonable because of the very large specific surface area of the aggregate, the large permeability of cement paste during the first week after production, and the small traveling distance of water. The latter was quantified by Garboczi and Bentz (1997), who applied an analytical formula from Lu and Torquato (1992) to predict the volume fraction of cement paste which is within a distance r around the aggregate. Considering a typical aggregate grading curve, idealizing aggregate as spherical, and considering that 75% of the concrete

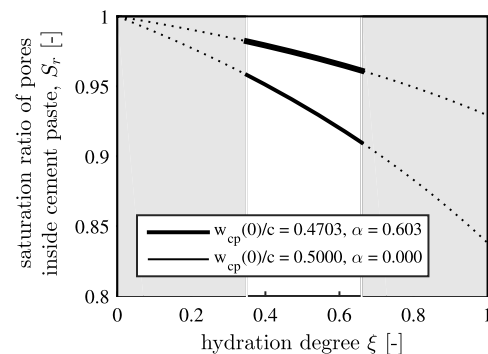


Fig. 13. Evolution of saturation ratio of cement paste matrix as a function of hydration degree, according to the modified Powers–Acker–Hansen model: evaluation of Eq. (49) for $w_{cp}(0)/c = 0.4703$ as well as for water filling extent $\alpha = 0.603$ (present analysis) and $\alpha = 0$ (no internal curing within air-exposed sample); the central nonshaded domain refers to the experimentally investigated interval of hydration degrees $\xi \in [0.32, 0.65]$

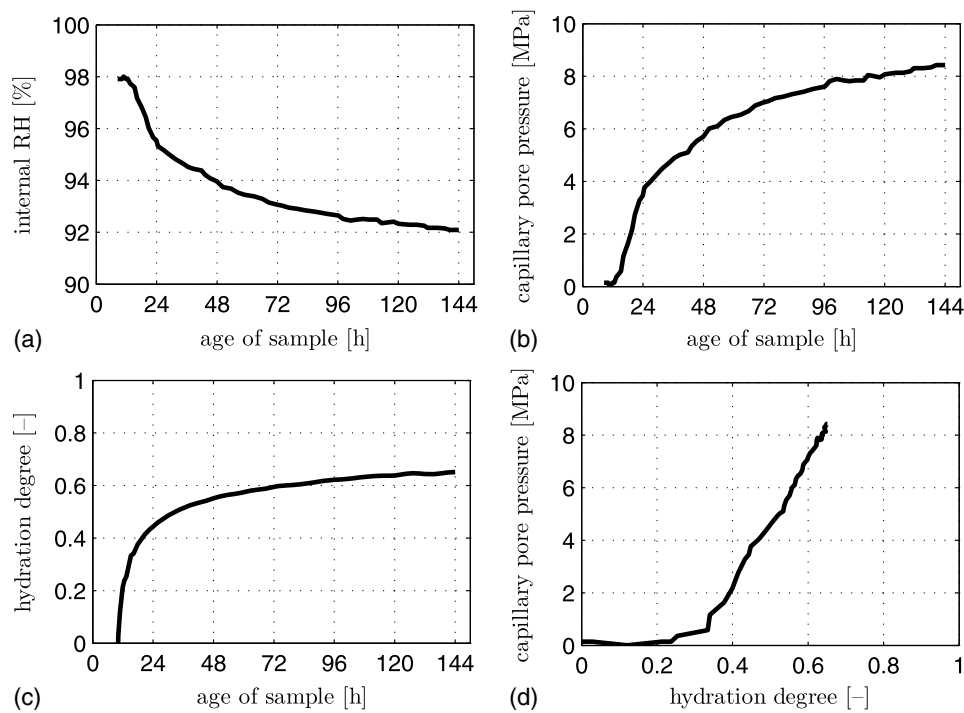


Fig. 14. Experimental data from Lura et al. (2003) on cement paste with $w/c = 0.37$: (a) internal relative humidity as a function of material age; (b) capillary pressure as a function of material age; (c) hydration degree as a function of material age; (d) capillary pressure as a function of hydration degree

volume consists of aggregate, they showed that almost all the cement paste is located within the first $100 \mu\text{m}$ around the aggregate. Similar conclusions were drawn by Rangaraju et al. (2010), who found that the mean interaggregate spacing typically ranges between 60 and $160 \mu\text{m}$.

Suction of water from aggregate to the cement paste matrix might well be driven by shrinkage-related underpressure in the cement paste matrix. In this context, Lura et al. (2003) measured the evolution of internal relative humidity during the first week after production in a cement paste exhibiting $w/c = 0.37$ [Fig. 14(a)]. Considering that the salt content in the porewater was responsible for the decrease of internal relative humidity from 100 to 98% , and combining Kelvin and Laplace laws, Lura et al. quantified the evolution of capillary pressure [Fig. 14(b)]. Finally, Lura et al. measured the evolution of hydration degree by means of calorimetry [Fig. 14(c)]. Combining these data to produce a parameter plot showing capillary pressure as a function of hydration degree, with the age of the material as the parameter, delivers the very remarkable result that capillary pressure increases linearly with increasing hydration degree once the hydration degree becomes greater than 30% [Fig. 14(d)].

It could be speculated that the results by Lura et al. (2003) [Fig. 14(d)] for neat cement pastes without internal curing apply qualitatively also to the mortars and concretes exhibiting internal curing studied in this paper. This would suggest that the kinetics of water migration from the aggregate into the cement paste matrix could be governed by the increase of capillary pressure resulting from self-desiccation, at least in the regime investigated in this paper of hydration degrees from 30 to 65% .

In the context of a reductionist approach, one constant value of the void-filling extent α was used for all four investigated mortars and concretes. Alternatively, the effective water:cement ratio of cement paste could be treated as a fitting parameter for the reanalysis of every 3-min creep test. The optimal $w_{cp}(\xi)/c$ values should then

be identified such that model outputs agree with experimental data in the best possible fashion. Corresponding optimal $w_{cp}(\xi)/c$ values related to more than 150 tests per tested mortar and concrete specimen resolve the relationship between the effective water:cement ratio of cement paste and the hydration degree in a pointwise manner. The result is—in very good approximation—a linear relationship such as that described by Eq. (2). In addition, the fitting results allow for identification of one specific value of the void-filling extent for each of the two tested mortars and concretes (Table 7). These four optimal values of the void-filling extent allow for the following interpretations:

1. The void-filling extent of mortars is larger than that of concretes exhibiting the same nominal water:cement mass ratio. This suggests that the void-filling extent might increase with increasing surface area of the aggregate. Mortar sand, specifically, has smaller particle sizes than concrete aggregate, so that a specific mass of mortar sand has a larger surface area than does the same mass of concrete aggregate.
2. The void-filling extent increases with decreasing nominal water:cement mass ratio. This is consistent with the observation that shrinkage increases with decreasing initial water:cement mass ratio (e.g., Lura et al. 2003).

It is concluded that consideration of water migration related to constant void-filling extent is a first-order approximation.

Table 7. Void-Filling Extent Optimized Individually for the Four Tested Materials

Material	Void-filling extent α
Mortar #1	0.603
Mortar #2	0.612
Concrete #1	0.575
Concrete #2	0.585

Outlook

In the future, it will be interesting to

- Develop methods that allow for predicting the initial water uptake capacity of oven-dried aggregate;
- Perform hourly repeated 3-min creep tests on mortars and concretes with initially water-saturated sand and aggregate; and
- Develop experimental techniques that allow for direct confirmation of the water migration from aggregate to cement paste described in this paper, which are applicable also during the first 20 h after production, i.e., in the regime of hydration degrees smaller than 30%.

Conclusions

This paper presented an extension of the classical Powers hydration model with respect to internal curing, and checked the relevance of the latter through micromechanical upscaling of effective water: cement mass ratio–dependent cement paste creep functions, up to the levels of mortar/concrete. Remarkably, internal curing can be considered in terms of only two additional quantities: an aggregate-specific uptake capacity, and a cement paste–specific void-filling extent. Identifying these quantities for two types of oven-dried quartz aggregate and for one type of cement allowed for satisfactory prediction of numerous ultrashort-term creep tests on two mortars and two concretes (Figs. 8–11). Such creep tests directly deliver the hydration-dependent (nonaging) creep properties, and are also valid for medium-term creep tests on very old pastes (Irfan-ul-Hassan et al. 2016). Neglecting internal curing effects, i.e., initial water uptake through the aggregate followed by back-suction of this water from the aggregate domain to that of the

maturing cement paste, clearly does not allow for satisfactory micromechanical prediction of the creep properties at the mortar and concrete level, as is quantified in Table 2 and illustrated in Fig. 15, which shows predictions based on $w_a(0)/a = \alpha = f_{air} = 0$ while keeping all other input variables as defined in this paper. Obviously, the creep response predicted by the micromechanical model (Fig. 2) would be too soft under these conditions. It is also illustrative to quantify the degree of hydration when the back-suction of water from aggregate to the cement paste is complete, simply because no water is left in the aggregate. To this end, $w_{cp}(\xi)/c$ in Eq. (10) is set equal to w/c and the resulting expression is solved for hydration degree ξ

$$\xi^* = \frac{\frac{w_a(0)}{a}(a/c)\{20 + 63[w/c - \frac{w_a(0)}{a}(a/c)]\}}{\alpha\{1.051 + 3.31[w/c - \frac{w_a(0)}{a}(a/c)]\}} \quad (50)$$

Notably, the creep tests analyzed herein refer to hydration degrees smaller than ξ^* [Figs. 8(b), 9(b), 10(b), and 11(b)].

The method described herein, showing how to integrate internal curing events into micromechanical modeling of concrete, in particular concerning creep, can be straightforwardly extended to aging creep behavior based on earlier contributions such as those by Scheiner and Hellmich (2009) or Sanahuja (2013).

Another obvious extension concerns the deeper reasons for the dependencies of the creep properties of cement paste on the water: cement mass ratio (Fig. 4), which may be deciphered through micromechanical resolution to the level of the hydrates (Königsberger et al. 2016), or even to the level of lubricating water layers between calcium silicate sheets (Pellenq et al. 2009; Sanahuja and Dormieux 2010; Shahidi et al. 2014, 2016a, b; Vandamme et al. 2015).

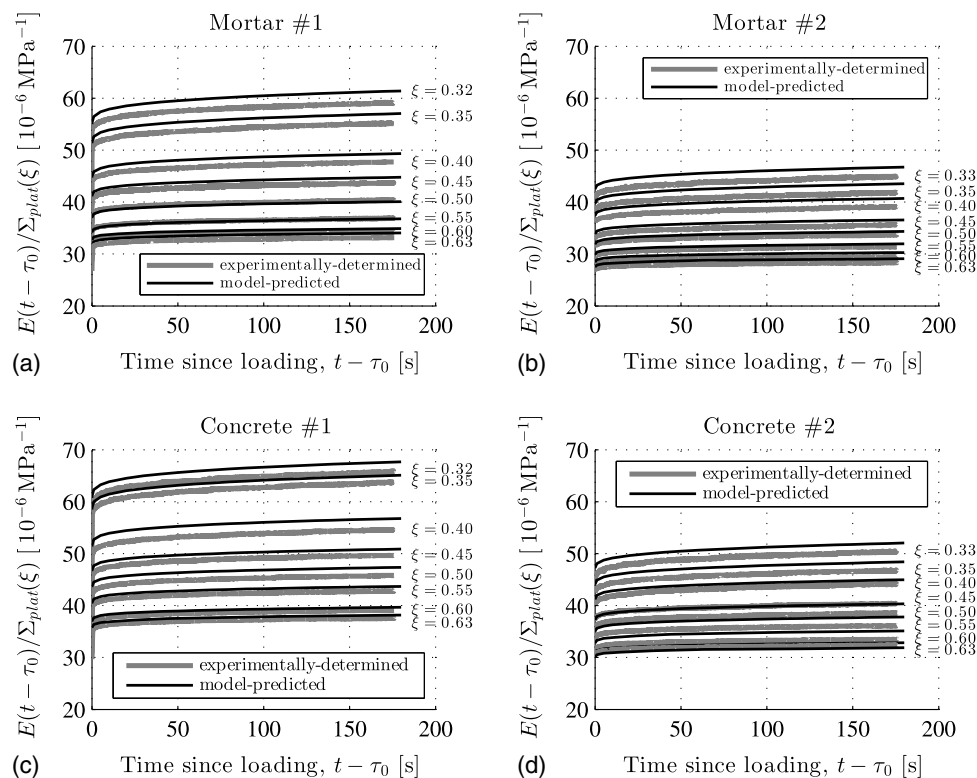


Fig. 15. Comparison of experimentally determined and model-predicted plateau stress–normalized strains using nominal compositions as input (Table 1) at hydration degrees according to Eq. (19), for the corresponding load plateaus see Eq. (20): (a) Mortar #1; (b) Mortar #2; (c) Concrete #1; (d) Concrete #2; model-predicted strains overestimate experimentally measured strains (Table 2)

Appendix. Analytical Expressions Facilitating Upscaling in LC Space

Upscaling of the creep behavior to the larger scales of mortar or concrete was performed in the LC space, according to the analytical formulae described in this appendix. An isotropic fourth-order tensor, \mathbb{G} , can be decomposed into a volumetric part and a deviatoric part as $\mathbb{G} = G^{vol}\mathbb{1}^{vol} + G^{dev}\mathbb{1}^{dev}$, where G^{vol} and G^{dev} , respectively, are the (scalar) volumetric and deviatoric components of the tensor, and $\mathbb{1}^{vol}$ and $\mathbb{1}^{dev}$ are the volumetric and deviatoric parts of the fourth-order identity tensor $\mathbb{1}$, defined as $I_{ijkl} = 1/2(\delta_{ik}\delta_{jl} + \delta_{il}\delta_{jk})$, $\mathbb{1}^{vol} = 1/3(\mathbf{1} \otimes \mathbf{1})$, and $\mathbb{1}^{dev} = \mathbb{1} - \mathbb{1}^{vol}$, respectively, where $\mathbf{1}$ denotes the second-order identity tensor with components equal to the Kronecker delta δ_{ij} , namely $\delta_{ij} = 1$ for $i = j$, and 0 otherwise. They satisfy $\mathbb{1}^{vol}:\mathbb{1}^{vol} = \mathbb{1}^{vol}$, $\mathbb{1}^{dev}:\mathbb{1}^{dev} = \mathbb{1}^{dev}$, and $\mathbb{1}^{vol}:\mathbb{1}^{dev} = \mathbb{1}^{dev}:\mathbb{1}^{vol} = 0$.

The collection of analytical formulas is started with the LC-transformed Hill tensors for spherical inclusions embedded in an infinite cement matrix with quasi-elastic stiffness \mathbb{R}_{cp}^* , occurring in concentration and stiffness expressions of Eq. (14). The Hill tensor is

$$\mathbb{P}_{sph}^*(p) = \mathbb{S}_{sph}^*(p) : [\mathbb{R}_{cp}^*(p)]^{-1} \quad (51)$$

where \mathbb{S}_{sph}^* = LC-transformed Eshelby tensor of a spherical inclusion embedded in an infinite cement paste matrix. The LC-transformed Eshelby tensor \mathbb{S}_{sph}^* is isotropic, and its volumetric and deviatoric components are (Zaoui 2002; Hellmich et al. 2004)

$$\begin{aligned} S_{sph}^{*,vol}(p) &= \frac{3k_{cp}^*(p)}{3k_{cp}^*(p) + 4\mu_{cp}^*(p)}, \\ S_{sph}^{*,dev}(p) &= \frac{6k_{cp}^*(p) + 2\mu_{cp}^*(p)}{5k_{cp}^*(p) + 4\mu_{cp}^*(p)} \end{aligned} \quad (52)$$

Next, the expressions for the homogenized quasi-elastic stiffness tensor \mathbb{R}_{hom}^* are discussed. For mortar or concrete, insertion of the LC-transformed Eshelby tensor expressions [Eq. (52)] into Eq. (51), and further insertion of the obtained Hill tensor, together with the vanishing quasi-elastic stiffnesses of air and the available quasi-elastic stiffness of quartz [Eq. (16)], into the expression for the quasi-elastic stiffness of the homogenized mortar or concrete [Eq. (14)], yields scalar expressions for the LC-transformed bulk and shear moduli

$$\begin{aligned} k_{hom}^*(p) &= [f_{cp}k_{cp}^*(p) + f_{agg}k_{agg}A_{\infty,agg}^{*,vol}(p)] \\ &\quad \times [f_{cp} + f_{agg}A_{\infty,agg}^{*,vol}(p) + f_{air}A_{\infty,air}^{*,vol}(p)]^{-1}, \\ \mu_{hom}^*(p) &= [f_{cp}\mu_{cp}^*(p) + f_{agg}\mu_{agg}A_{\infty,agg}^{*,dev}(p)] \\ &\quad \times [f_{cp} + f_{agg}A_{\infty,agg}^{*,dev}(p) + f_{air}A_{\infty,air}^{*,dev}(p)]^{-1} \end{aligned} \quad (53)$$

where $A_{\infty,agg}^{*,vol}$, $A_{\infty,agg}^{*,dev}$, $A_{\infty,air}^{*,vol}$, and $A_{\infty,air}^{*,dev}$ are denoting LC-transformed volumetric and deviatoric components of the Eshelby problem-related strain concentration tensors for quartz aggregate and air. For air, the volumetric and deviatoric components of the strain concentration tensor can be written as

$$\begin{aligned} A_{\infty,air}^{*,vol}(p) &= [1 - S_{sph}^{*,vol}(p)]^{-1}, \\ A_{\infty,air}^{*,dev}(p) &= [1 - S_{sph}^{*,dev}(p)]^{-1} \end{aligned} \quad (54)$$

For quartz, these components are

$$\begin{aligned} A_{\infty,agg}^{*,vol}(p) &= \left[1 + S_{sph}^{*,vol}(p) \frac{k_{agg} - k_{cp}^*(p)}{k_{cp}^*(p)} \right]^{-1}, \\ A_{\infty,agg}^{*,dev}(p) &= \left[1 + S_{sph}^{*,dev}(p) \frac{\mu_{agg} - \mu_{cp}^*(p)}{\mu_{cp}^*(p)} \right]^{-1} \end{aligned} \quad (55)$$

Acknowledgments

The authors cordially thank for valuable help the laboratory staff of the Institute of Mechanics of Materials and Structures, TU Wien—Vienna University of Technology. The first author also thanks the Higher Education Commission (HEC) Pakistan and the University of Engineering and Technology, Lahore, Pakistan, for their support.

Notation

The following symbols are used in this paper:

- $\mathbf{1}$ = second-order identity tensor;
- $A_{\infty,agg}^{*,dev}$ = LC-transformed deviatoric component of Eshelby problem-related strain concentration tensor of aggregate;
- $A_{\infty,air}^{*,dev}$ = LC-transformed deviatoric component of Eshelby problem-related strain concentration tensor of air;
- $A_{\infty,agg}^{*,vol}$ = LC-transformed volumetric component of Eshelby problem-related strain concentration tensor of aggregate;
- $A_{\infty,air}^{*,vol}$ = LC-transformed volumetric component of Eshelby problem-related strain concentration tensor of air;
- a = mass of aggregate;
- a/c = aggregate:cement mass ratio;
- c = mass of cement paste;
- d = a material constant equal to $w_{cp}(0)/c$;
- d_{max} = maximum diameter of aggregate;
- \mathbf{E} = macroscopic strain tensor;
- E = macroscopic uniaxial strain;
- $E_{c,cp}$ = Young's creep modulus of cement paste;
- E_{cp} = Young's elastic modulus of cement paste;
- E^{exp} = experimentally determined macroscopic uniaxial strain;
- E^{pred} = model-predicted macroscopic uniaxial strain;
- F_{plat} = plateau force;
- f_{agg} = volume fraction of aggregate;
- f_{agg}^{no-air} = volume fraction of aggregate without entrapped air;
- f_{air} = volume fraction of air;
- f_{air}^{cp} = cement paste-related volume fraction of air;
- f_{cap}^{cp} = cement paste-related volume fraction of capillary pores;
- f_{clin}^{cp} = cement paste-related volume fraction of clinker;
- f_{cp} = volume fraction of cement paste;
- f_{cp}^{no-air} = volume fraction of cement paste without entrapped air;
- f_{gel}^{cp} = cement paste-related volume fraction of gel pores;
- $f_{H_2O}^{cp}$ = cement paste-related volume fraction of liquid water;
- f_{hyd}^{cp} = cement paste-related volume fraction of hydration products;

f_{pores}^{cp} = cement paste-related volume fraction of pores;
 f_{void}^{cp} = cement paste-related volume fraction of voids;
 f_{water}^{cp} = cement paste-related volume fraction of liquid water in capillary pores and voids;
 \mathbb{G} = auxiliary isotropic fourth-order tensor;
 G^{vol}, G^{dev} = volumetric and deviatoric components of \mathbb{G} ;
 \mathbb{I} = fourth-order identity tensor;
 $\mathbb{I}^{vol}, \mathbb{I}^{dev}$ = volumetric and deviatoric parts of \mathbb{I} ;
 \mathbb{J}_{hom} = homogenized fourth-order tensorial creep function;
 k = material constant equal to rate of w_{cp}/c ;
 k_{agg} = bulk modulus of aggregate;
 k_{air} = bulk modulus of air;
 k_{cp} = bulk modulus of cement paste;
 k_{hom} = bulk modulus of mortar or concrete;
 \mathbb{P}_{sph}^* = LC-transformed Hill tensor of spherical inclusions embedded in an infinite cement paste matrix;
 p = complex variable in the LC domain;
 \mathbb{R}_{agg}^* = LC-transformed fourth-order relaxation tensor function of aggregate;
 \mathbb{R}_{air}^* = LC-transformed fourth-order relaxation tensor function of air;
 \mathbb{R}_{cp}^* = LC-transformed fourth-order relaxation tensor function of cement paste;
 \mathbb{R}_{hom}^* = LC-transformed fourth-order relaxation tensor function of mortar or concrete;
 S_r = saturation ratio of cement paste;
 S_{sph}^* = LC-transformed Eshelby tensor of spherical inclusion embedded in an infinite cement paste matrix;
 $S_{sph}^{*,vol}, S_{sph}^{*,dev}$ = volumetric and deviatoric components of S_{sph}^* ;
 t = chronological time;
 t_{ref} = reference time, $t_{ref} = 1 \text{ d} = 86\,400 \text{ s}$;
 V_c = volume of cement;
 V_{cp} = volume of cement paste;
 V_{void} = volume of voids;
 V_w = volume of water;
 ν_{cp} = Poisson's ratio of cement paste;
 w = total water mass;
 w_a = water absorbed into aggregate;
 $w_a(0)/a$ = initial water:aggregate mass ratio;
 w_{cp} = water residing in cement paste;
 $w_{cp}(0)/c$ = initial value of the effective water:cement mass ratio;
 w_{cp}/c = effective water:cement mass ratio;
 w/c = (nominal) water:cement mass ratio;
 α = water-filling extent of shrinkage induced voids in cement paste;
 β_{cp} = power-law creep exponent for cement paste;
 $\Gamma(\cdot)$ = gamma function of real quantity (\cdot);
 δ_{ij} = Kronecker delta;
 \mathcal{E} = prediction error;
 μ_{agg} = shear modulus of aggregate;
 μ_{air} = shear modulus of air;
 μ_{cp} = shear modulus of cement paste;
 μ_{hom} = shear modulus of mortar or concrete;
 ξ = hydration degree;
 ξ^* = hydration degree at which all aggregate-absorbed water is sucked to cement paste;
 ρ_{agg} = mass density of aggregate;

ρ_{clin} = mass density of cement clinker;
 ρ_{H_2O} = mass density of water;
 ρ_{hyd} = mass density of hydrates;
 Σ = macroscopic stress tensor;
 Σ_{plat} = plateau stress;
 τ = time instant during creep test;
 τ_0 = time instant at start of loading ramp;
 $(\cdot)^*$ = Laplace–Carson transform of quantity (\cdot);
 $(\hat{\cdot})$ = Laplace transform of quantity (\cdot);
 $(\dot{\cdot})$ = time derivative of quantity (\cdot);
 \cdot = inner product;
 \times = multiplication; and
 $:=$ = second-order tensor contraction.

References

- Acker, P. (2001). "Micromechanical analysis of creep and shrinkage mechanisms." *6th Int. Conf. on Creep, Shrinkage and Durability Mechanics of Concrete and Other Quasi-Brittle Materials, CONCREEP@MIT*, F.-J. Ulm, Z. Bažant, and F. Wittmann, eds., Elsevier, Amsterdam, Netherlands.
- Acker, P., and Ulm, F.-J. (2001). "Creep and shrinkage of concrete: Physical origins and practical measurements." *Nucl. Eng. Des.*, 203(2–3), 143–158.
- Atrushi, D. (2003). "Tensile and compressive creep of early age concrete: Testing and modelling." Ph.D. thesis, Norwegian Univ. of Science and Technology, Trondheim, Norway.
- Barthélémy, J.-F., and Dormieux, L. (2003). "Détermination du critère de rupture macroscopique d'un milieu poreux par homogénéisation non linéaire [Determination of a macroscopic failure criterion for porous materials using nonlinear homogenization]." *Comptes Rendus Mécanique*, 331(4), 271–276.
- Bass, J. (2013). *Elasticity of minerals, glasses, and melts*, American Geophysical Union, Washington, DC.
- Baweja, S., Dvorak, G. J., and Bažant, Z. P. (1998). "Triaxial composite model for basic creep of concrete." *J. Eng. Mech.*, 10.1061/(ASCE)0733-9399(1998)124:9(959), 959–965.
- Bažant, Z. P., Asghari, A., and Schmidt, J. (1976). "Experimental study of creep of hardened Portland cement paste at variable water content." *Matériaux et Constructions*, 9(4), 279–290.
- Bažant, Z. P., Hubler, M. H., and Yu, Q. (2011). "Pervasiveness of excessive segmental bridge deflections: Wake-up call for creep." *ACI Struct. J.*, 108(6), 766–774.
- Bažant, Z. P., Yu, Q., and Li, G. (2012). "Excessive long-time deflections of prestressed box girders. I: Record-span bridge in Palau and other paradigms." *J. Struct. Eng.*, 10.1061/(ASCE)ST.1943-541X.0000487, 676–686.
- Bentz, D., Lura, P., and Roberts, J. (2005). "Mixture proportioning for internal curing." *Concr. Int.*, 27(2), 35–40.
- Bernard, O., Ulm, F.-J., and Lemarchand, E. (2003). "A multiscale micromechanics-hydration model for the early-age elastic properties of cement-based materials." *Cem. Concr. Res.*, 33(9), 1293–1309.
- Beurthey, S., and Zaoui, A. (2000). "Structural morphology and relaxation spectra of viscoelastic heterogeneous materials." *Eur. J. Mech. A. Solids*, 19(1), 1–16.
- Boulay, C., Crespini, M., Delsaute, B., and Staquet, S. (2012). "Monitoring of the creep and the relaxation behaviour of concrete since setting time. Part 1: Compression." *Int. Conf. on Numerical Modeling Strategies for Sustainable Concrete Structures (SSCS)*, Aix-en-Provence, France, 1–10.
- Briffaut, M., Benboudjema, F., Torrenti, J.-M., and Nahas, G. (2012). "Concrete early age basic creep: Experiments and test of rheological modelling approaches." *Constr. Build. Mater.*, 36, 373–380.
- Delsaute, B., Staquet, S., and Boulay, C. (2012). "Monitoring of the creep and the relaxation behaviour of concrete since setting time. Part 2: Tension." *Int. Conf. on Numerical Modeling Strategies for*

- Sustainable Concrete Structures (SSCS)*, Aix-en-Provence, France, 1–11.
- Garboczi, E., and Bentz, D. (1997). “Analytical formulas for interfacial transition zone properties.” *Adv. Cem. Based Mater.*, 6(3–4), 99–108.
- Gaver, D. (1966). “Observing stochastic processes, and approximate transform inversion.” *Oper. Res.*, 14(3), 444–459.
- Ghabezloo, S. (2010). “Association of macroscopic laboratory testing and micromechanics modelling for the evaluation of the poroelastic parameters of a hardened cement paste.” *Cem. Concr. Res.*, 40(8), 1197–1210.
- Hellmich, C., Barthélémy, J.-F., and Dormieux, L. (2004). “Mineral-collagen interactions in elasticity of bone ultrastructure—a continuum micromechanics approach.” *Eur. J. Mech. A. Solids*, 23(5), 783–810.
- Hellmich, C., and Mang, H. (2005). “Shotcrete elasticity revisited in the framework of continuum micromechanics: From submicron to meter level.” *J. Mater. Civ. Eng.*, 10.1061/(ASCE)0899-1561(2005)17:3(246), 246–256.
- Irfan-ul-Hassan, M., Pichler, B., Reihnsner, R., and Hellmich, C. (2016). “Elastic and creep properties of young cement paste, as determined from hourly repeated minute-long quasi-static tests.” *Cem. Concr. Res.*, 82, 36–49.
- Jensen, O., and Hansen, P. (2001). “Water-entrained cement-based materials. I: Principles and theoretical background.” *Cem. Concr. Res.*, 31(4), 647–654.
- Jensen, O., and Lura, P. (2006). “Techniques and materials for internal water curing of concrete.” *Mater. Struct.*, 39(9), 817–825.
- Justs, J., Wyrzykowski, M., Bajare, D., and Lura, P. (2015). “Internal curing by superabsorbent polymers in ultra-high performance concrete.” *Cem. Concr. Res.*, 76, 82–90.
- Königsberger, M., Irfan-ul Hassan, M., Pichler, B., and Hellmich, C. (2016). “Downscaling-based identification of non-aging power-law creep of cement hydrates.” *J. Eng. Mech.*, 10.1061/(ASCE)EM.1943-7889.0001169, 04016106.
- Laplante, P. (2003). “Propriétés mécaniques de bétons durcissants: Analyse comparée des bétons classique et à très hautes performances [Mechanical properties of hardening concrete: A comparative analysis of ordinary and high performance concretes].” Ph.D. thesis, Ecole Nationale des Ponts et Chaussées, Paris.
- Laws, N., and McLaughlin, R. (1978). “Self-consistent estimates for the viscoelastic creep compliances of composite materials.” *Proc. Royal Soc. London A*, 359(1697), 251–273.
- Lu, B., and Torquato, S. (1992). “Nearest-surface distribution functions for polydispersed particle systems.” *Phys. Rev. A*, 45(8), 5530–5544.
- Lura, P., Jensen, O., and van Breugel, K. (2003). “Autogenous shrinkage in high-performance cement paste: An evaluation of basic mechanisms.” *Cem. Concr. Res.*, 33(2), 223–232.
- Pellenq, R.-M., et al. (2009). “A realistic molecular model of cement hydrates.” *PNAS*, 106(38), 16102–16107.
- Pichler, B., et al. (2013). “Effect of gel-space ratio and microstructure on strength of hydrating cementitious materials: An engineering micromechanics approach.” *Cem. Concr. Res.*, 45, 55–68.
- Pichler, B., and Hellmich, C. (2011). “Upscaling quasi-brittle strength of cement paste and mortar: A multi-scale engineering mechanics model.” *Cem. Concr. Res.*, 41(5), 467–476.
- Pichler, B., Hellmich, C., and Eberhardsteiner, J. (2009). “Spherical and acicular representation of hydrates in a micromechanical model for cement paste: Prediction of early-age elasticity and strength.” *Acta Mech.*, 203(3), 137–162.
- Pichler, B., Scheiner, S., and Hellmich, C. (2008). “From micron-sized needle-shaped hydrates to meter-sized shotcrete tunnel shells: Micromechanical upscaling of stiffness and strength of hydrating shotcrete.” *Acta Geotech.*, 3(4), 273–294.
- Powers, T., and Brownyard, T. (1946). “Studies of the physical properties of hardened Portland cement paste.” *J. Proc., Am. Concr. Inst.*, 43(9), 101–132.
- Rangaraju, P., Olek, J., and Diamond, S. (2010). “An investigation into the influence of inter-aggregate spacing and the extent of the ITZ on properties of Portland cement concretes.” *Cem. Concr. Res.*, 40(11), 1601–1608.
- Read, W. (1950). “Stress analysis for compressible viscoelastic media.” *J. Appl. Phys.*, 21(7), 671–674.
- Rossi, P., Godart, N., Robert, J., Gervais, J., and Bruhat, D. (1994). “Investigation of the basic creep of concrete by acoustic emission.” *Mater. Struct.*, 27(9), 510–514.
- Rossi, P., Tailhan, J.-L., Le Maou, F., Gaillet, L., and Martin, E. (2012). “Basic creep behavior of concretes investigation of the physical mechanisms by using acoustic emission.” *Cem. Concr. Res.*, 42(1), 61–73.
- Sanahuja, J. (2013). “Effective behaviour of ageing linear viscoelastic composites: Homogenization approach.” *Int. J. Solids Struct.*, 50(19), 2846–2856.
- Sanahuja, J., and Dormieux, L. (2010). “Creep of a C-S-H gel: A micro-mechanical approach.” *Ann. Braz. Acad. Sci.*, 82(1), 25–41.
- Sanahuja, J., Dormieux, L., and Chanvillard, G. (2007). “Modelling elasticity of a hydrating cement paste.” *Cem. Concr. Res.*, 37(10), 1427–1439.
- Scheiner, S., and Hellmich, C. (2009). “Continuum microviscoelasticity model for ageing basic creep of early-age concrete.” *J. Eng. Mech.*, 10.1061/(ASCE)0733-9399(2009)135:4(307), 307–323.
- Shahidi, M., Pichler, B., and Hellmich, C. (2014). “Viscous interfaces as source for material creep: A continuum micromechanics approach.” *Eur. J. Mech. A. Solids*, 45, 41–58.
- Shahidi, M., Pichler, B., and Hellmich, C. (2016a). “Interfacial micromechanics assessment of classical rheological models. I: Single interface size and viscosity.” *J. Eng. Mech.*, 10.1061/(ASCE)EM.1943-7889.0001012, 04015092.
- Shahidi, M., Pichler, B., and Hellmich, C. (2016b). “Interfacial micromechanics assessment of classical rheological models. II: Multiple interface sizes and viscosities.” *J. Eng. Mech.*, 10.1061/(ASCE)EM.1943-7889.0001013, 04015093.
- Sips, R. (1951). “General theory of deformation of viscoelastic substances.” *J. Polymer Sci.*, 7(2–3), 191–205.
- Tamtsia, B., and Beaudoin, J. (2000). “Basic creep of hardened cement paste. A re-examination of the role of water.” *Cem. Concr. Res.*, 30(9), 1465–1475.
- Tamtsia, B., Beaudoin, J., and Marchand, J. (2004). “The early age short-term creep of hardening cement paste: Load-induced hydration effects.” *Cem. Concr. Res.*, 26(5), 481–489.
- Ulm, F. J., Constantinides, G., and Heukamp, F. H. (2004). “Is concrete a poromechanics materials?—A multiscale investigation of poroelastic properties.” *Mater. Struct.*, 37(1), 43–58.
- Vandamme, M., Bažant, Z., and Keten, S. (2015). “Creep of lubricated layered nano-porous solids and application to cementitious materials.” *J. Nanomech. Micromech.*, 10.1061/(ASCE)NM.2153-5477.0000102, 04015002.
- Vandamme, M., and Ulm, F.-J. (2009). “Nanogranular origin of concrete creep.” *Proc. Nat. Acad. Sci. U.S.A.*, 106(26), 10552–10557.
- Vandamme, M., and Ulm, F.-J. (2013). “Nanoindentation investigation of creep properties of calcium silicate hydrates.” *Cem. Concr. Res.*, 52, 38–52.
- Wyrzykowski, M., Lura, P., Pesavento, F., and Gawin, D. (2011). “Modelling of internal curing in maturing mortar.” *Cem. Concr. Res.*, 41(12), 1349–1356.
- Zaoui, A. (2002). “Continuum micromechanics: Survey.” *J. Eng. Mech.*, 10.1061/(ASCE)0733-9399(2002)128:8(808), 808–816.
- Zhang, Q., Roy, R., Vandamme, M., and Zuber, B. (2014). “Long-term creep properties of cementitious materials: Comparing microindentation testing with macroscopic uniaxial compressive testing.” *Cem. Concr. Res.*, 58, 89–98.
- Zhutovsky, S., and Kovler, K. (2012). “Effect of internal curing on durability-related properties of high performance concrete.” *Cem. Concr. Res.*, 42(1), 20–26.